Modeling and Simulation of the Portevin-Le Chatelier Effect

Albrecht Bertram[1], **Thomas Böhlke**[1,2], **Carina Brüggemann**[*1], **Yuri Estrin**[3], and **Mikhail Lebyodkin**[3]

[1] Institut für Mechanik, Otto-von-Guericke-Universität Magdeburg, Postfach 4120, D-39016 Magdeburg, Germany
[2] Institut für Mechanik, Fachbereich Maschinenbau, Universität Kassel, D-34109 Kassel, Germany
[3] Institut für Werkstoffkunde und Werkstofftechnik, Technische Universität Clausthal, D-38678 Clausthal-Zellerfeld, Germany

During deformation of an Al-Mg alloy (AA5754) dynamic strain aging occurs in a certain range of temperatures and strain-rates. An extreme manifestation of this phenomenon, usually referred to as the Portevin-Le Chatelier (PLC) effect, consists in the occurrence of strain localisation bands accompanied with discontinuous yielding. The PLC effect stems from dynamic dislocation-solute interactions and results in negative strain-rate sensitivity of the flow stress. The PLC effect is detrimental to the surface quality of sheet metals and also affects the ductility of the material. Since the appearance of the effect strongly depends on the triaxiality of the stress state, three-dimensional finite element simulations are necessary in order to optimize metal forming operations. We present a geometrically nonlinear material model which reproduces the main features of the PLC effect. The material parameters were identified based on experimental data from tensile tests. Special emphasis was put on the critical strain for the onset of PLC effect, ε_c, and the statistical characteristics of the stress drop distribution.

1 Experimental findings

Polycrystalline flat specimens (gage length 21mm, width 5.1mm, thickness 1.55mm) were manufactured from an Al-Mg alloy (AA5754). All samples were cut from sheet materials with the tensile axis chosen in the rolling direction. After grinding and polishing, the specimens were annealed for two hours at 400°C and quenched in water. Tensile tests were performed at room temperature with four different imposed strain rates between $2 \cdot 10^{-5}\mathrm{s}^{-1}$ and $6 \cdot 10^{-3}\mathrm{s}^{-1}$. The experimental stress-strain curves are shown in Fig. 1 (left).

2 Modeling of the PLC effect

In the following, an isotropic elastic viscoplastic material model is formulated. For small elastic deformations Hooke's law is given by

$$\boldsymbol{\tau} = \mathbb{C}[\mathbf{E}_e^A], \qquad \mathbb{C} \cong \lambda \mathbf{I} \otimes \mathbf{I} + 2G\mathbb{I}^S, \qquad \mathbf{E}_e^A = \frac{1}{2}(\mathbf{I} - \mathbf{B}_e^{-1}) \cong \frac{1}{2}(\mathbf{B}_e - \mathbf{I}), \tag{1}$$

where the Kirchhoff stress tensor $\boldsymbol{\tau}$ is connected to the elastic Almansi strain tensor $\mathbf{E}_e^A$ by the isotropic stiffness tensor $\mathbb{C}$. λ and G denote the Lamé coefficients and $\mathbf{B}_e = \mathbf{F}_e\mathbf{F}_e^{\mathsf{T}}$ the elastic left Cauchy Green tensor.

The viscoplastic behavior is given by a von Mises type flow rule for large plastic but small elastic deformations

$$-\frac{1}{2}\mathcal{L}_v(\mathbf{B}_e) = \mathrm{sym}(\mathbf{L}_p\mathbf{B}_e), \qquad \mathrm{sym}(\mathbf{L}_p\mathbf{B}_e) \approx \mathbf{D}_p, \qquad \mathbf{D}_p = \frac{3}{2}\frac{\dot{\varepsilon}_p}{\sigma}\boldsymbol{\tau}', \qquad \mathcal{L}_v(\mathbf{B}_e) = \dot{\mathbf{B}}_e - \mathbf{L}\mathbf{B}_e - \mathbf{B}_e\mathbf{L}^{\mathsf{T}}, \tag{2}$$

where $\dot{\varepsilon}_p = \sqrt{\frac{2}{3}} \parallel \mathbf{D}_p \parallel$ and $\sigma = \sqrt{\frac{3}{2}} \parallel \boldsymbol{\tau}' \parallel$. $\mathbf{L} = \dot{\mathbf{F}}\mathbf{F}^{-1}$ is the velocity gradient, where $\mathbf{F}$ is the defomation gradient. The prime denotes the symmetric and traceless part of a tensor.

On the microscale the PLC effect is produced by additional pinning of dislocations temporarily arrested at localized obstacles (forest dislocation junctions) by diffusing solutes. This mechanism is represented by the following scalar flow rule (Zhang et al., 2001)

$$\dot{\varepsilon}_p = \dot{\varepsilon}_o \exp\Big(\frac{\sigma - \sigma_d}{S} - P_1 C_s\Big), \qquad \sigma_d = d_1 + d_2\Big(1 - \exp\Big(-\frac{\varepsilon_p}{d_3}\Big)\Big), \qquad S = s_1 + s_2\sqrt{\varepsilon_p}. \tag{3}$$

σ_d describes the strain hardening and S the strain rate sensitivity of the flow stress. C_s is the concentration of solute atoms at pinned dislocations and depends on the accumulated plastic strain ε_p and the aging time t_a

$$C_s = \Big(1 - \exp\Big(-P_2\varepsilon_p^{\alpha}t_a^n\Big)\Big)C_m, \qquad \dot{t}_a = 1 - \frac{t_a}{t_w}, \qquad t_w = \frac{\Omega}{\dot{\varepsilon}_p}, \qquad \Omega = \omega_1 + \omega_2\varepsilon_p^{\beta}. \tag{4}$$

* Corresponding author: e-mail: carina.brueggemann@mb.uni-magdeburg.de, Phone: +49 (0)391 67-12076 Fax: +49 (0)391 67-12863

The aging time t_a is the time available to solute atoms to diffuse to dislocations. The rate of change of t_a depends on t_a and the waiting time t_w, the time a dislocation spends at localized obstacles before it unpins.

The material parameters used are as follows: $d_1 = 75.0$ MPa, $d_2 = 165.0$ MPa, $d_3 = 7.0 \cdot 10^{-2}$, $P_1 = 25.0, P_2 = 3.3$ $s^{1/3}$, $n = 1/3$, $\alpha = 0.44$, $\beta = 0.68$, $\omega_1 = 3.60 \cdot 10^{-7}$, $\omega_2 = 7.5 \cdot 10^{-4}$, $s_1 = 0.41$ MPa, $s_2 = 2.91$ MPa, $E = 70000$ MPa, $\nu = 0.3$, $\dot{\varepsilon}_o = 2.30 \cdot 10^{-7}$ s^{-1}. In order to solve the differential equations, the backward Euler method was used.

3 Comparison of experimental findings with numerical results

In Fig. 1 (left) the experimental findings are compared to the numerical results. The hardening behavior is reproduced well. The different types of serrations observed experimentally are recovered by the simulation. Detailed information about a statistical analysis of the PLC effect can be found in Lebyodkin et al. (2001) and Kubin et al. (2002). Without going into detail, it is only pointed out that the comparison of the statistical behavior, such as the stress drop distribution function and the correlation function, shows good agreement. Another characteristic feature is the critical strain ε_c, which is shown in Fig. 1 (right). In the high strain rate regime ε_c increases (normal behavior), while in the low strain rate regime it decreases with increasing $\dot{\varepsilon}$ (inverse behavior). The inverse branch is not recovered in the present version of the model using a monotonic strain dependence of Ω, but this can be rectified by using a non-monotonic function.

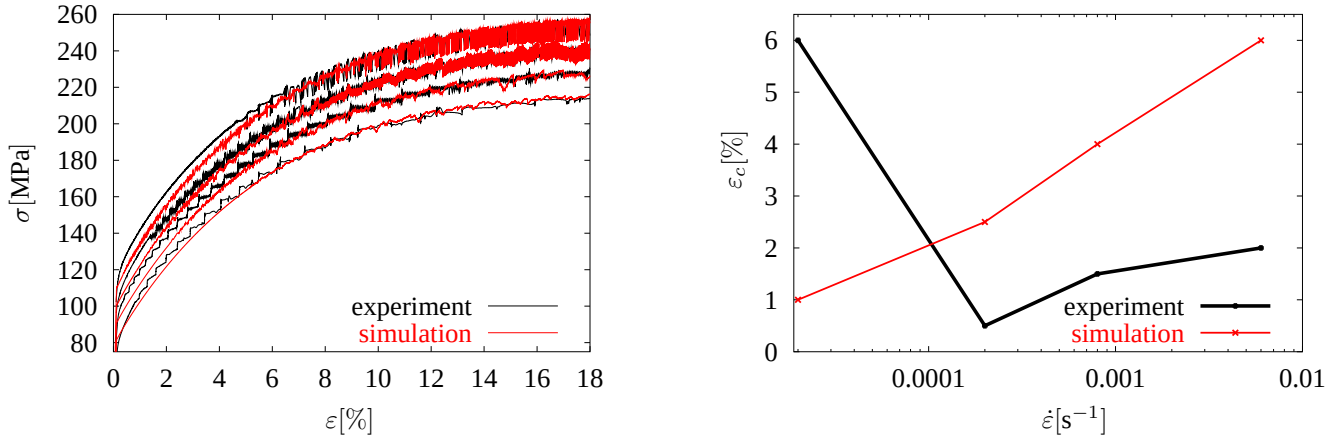

Fig. 1 Comparison of experimental findings with numerical results: σ vs. ε. The curves are deliberately shifted along the ordinate axis for clarity. The strain rate from the upper curve downwards are as follows: $2 \cdot 10^{-5}s^{-1}$[+30MPa], $2 \cdot 10^{-4}s^{-1}$[+20MPa] , $8 \cdot 10^{-4}s^{-1}$[+10MPa], $6 \cdot 10^{-3}s^{-1}$[+0MPa] (left) and ε_c vs. $\dot{\varepsilon}$ (right)

4 Conclusions

FE simulations were performed with a 3D isotropic, geometrically nonlinear PLC model. Material parameters were identified, and the results of the simulations were compared with experimental findings. The comparison of experiment with simulation shows good agreement for the strain hardening behavior and the statistical behavior of the stress drops for all strain rates.

Acknowledgements Financial support of Deutsche Forschungsgemeinschaft (DFG) is gratefully acknowledged. This project was also funded by the Graduiertenkolleg 828.

References

[1] Lebyodkin, M., Dunin-Barkowskii, L., and Lebedkina, T., Statistical and multifractal analysis of collective dislocation processes in the Portevin-Le Chatelier effect Physical, Mesomechanics **4**, 9 (2001).
[2] Kubin, L., Fressengeas, C., and Ananthakrishna, G., In Nabarro, F. and Duesbery, M., Collective Behaviour of Dislocations in Plasticity, Editors, Dislocations in Solids, 102 (2002).
[3] Zhang, S., McCormick, P., and Estrin, Y., The morphology of Portevin-Le Chatelier bands: finite element simulation for Al-Mg-Si, Acta. Mater. **49**, 1087 (2001).